Journal of the European Ceramic Society 21 (2001) 883–892

www.elsevier.com/locate/jeurceramsoc

Design and characterisation of a co-extruder to produce trilayer ceramic tubes semi-continuously

Z. Liang, S. Blackburn *

IRC in Materials for High Performance Applications and School of Chemical Engineering, The University of Birmingham, Edgbaston, Birmingham B15 2TT, UK

Received 20 June 2000; accepted 2 October 2000

Abstract

A co-extruder with three separate barrels operated by a single ram has been designed to produce trilayer tubes semi-continuously. A vital step in the design was to predict the pressure required to generate a sufficiently high extrudate velocity while being able to retain the extrudate integrity. A physically based model was used to predict the pressure drops in the co-extrusion process at three different extrusion velocities for five pastes with different rheological characteristics. In general, predicted and measured values were in good agreement. Other important aspects in the co-extruder design, such as velocity and pressure matching of different flow streams are also highlighted. Trilayer ceramic tubes were successfully produced from the designed co-extruder.

Keywords: Al_2O_3; Clays; Composites; Plasticity; Shaping; Extrusion

1. Introduction

Co-extrusion has been used to produce fine-scale complex ceramic objects.[1] These complex shapes were formed by first producing lay-up feed rod assemblies. When extruded the extrudates were re-assembled into a further feed rod and extruded again. This process was repeated to reduce the size and multiply the number of shaped patterns. Using similar procedures, multilayer ceramic tubes were produced by Liang and Blackburn.[2] While this process can produce very complex fine structures, it is time-consuming and lacks continuity because of the need to produce lay-ups before each extrusion. Therefore, this route has not yet been fully accepted by the ceramics industry.

Shannon and Blackburn[3] successfully designed a co-extruder which was able to produce laminates from two separate feeds, but with only a flat plate configuration. This highlights the difficulty with continuous processes in that each die can produce only one shape, but this is generally acceptable in the production environment.

In this work, a design procedure for developing a co-extruder with three separate barrels to produce trilayer ceramic tubes semi-continuously without the need for hand assembly is described.

Tube forming requires the pastes to flow through dies with a central mandrel. Conventionally a spider supports this mandrel and the paste must rejoin after passing the spider arms. This can lead to defects known as "lamination" which weaken the tube structure. Stronger tubes are formed, where no spider is used, but this normally requires a moving mandrel. In the design for trilayer tube extrusion, the problem of which design to use is compounded by the need to bring the three materials together to form three distinct and complete concentric layers. A compromise intermediate design was used whereby for each individual layer the paste was fed via a manifold around the pin.[4] This requires the pin to have a reasonably large diameter to prevent distortion from the tangential entry of the paste. The joining of the paste behind the pin could form a "lamination" in each layer, but by geometrically arranging the flows these laminations could be offset in the three layers minimizing the effect.

* Corresponding author.
E-mail address: s.blackburn@bham.ac.uk (S. Blackburn).

0955-2219/01/$ - see front matter
PII: S0955-2219(00)00292-2

2. Co-extruder, structural design

The design's aim was to produce trilayer tubes, the material for each layer being supplied from three separate barrels. To achieve this each material was to be applied consecutively around the central mandrel through a series of manifolds. By assuring constant volumetric displacement, the design made use of a single constant speed drive from a load frame, pushing the three plungers through a force transmission plate. Three removable steel balls were placed between the plungers and the top drive plate to tolerate any misalignment between the different plungers. The key aspects of the design are shown in Fig. 1.

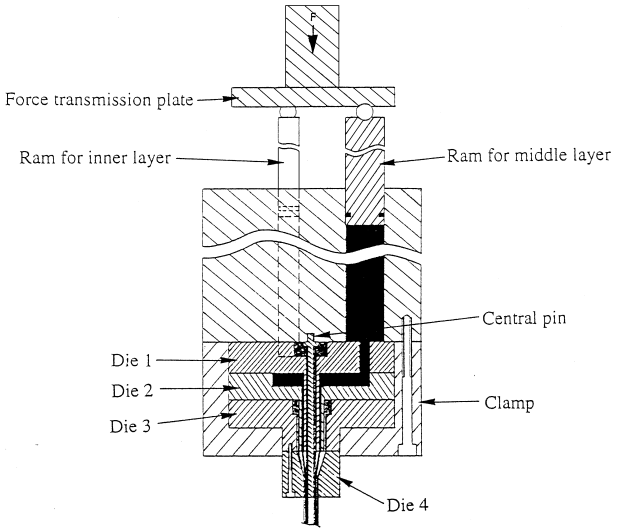

Fig. 1. The external view of the co-extruder.

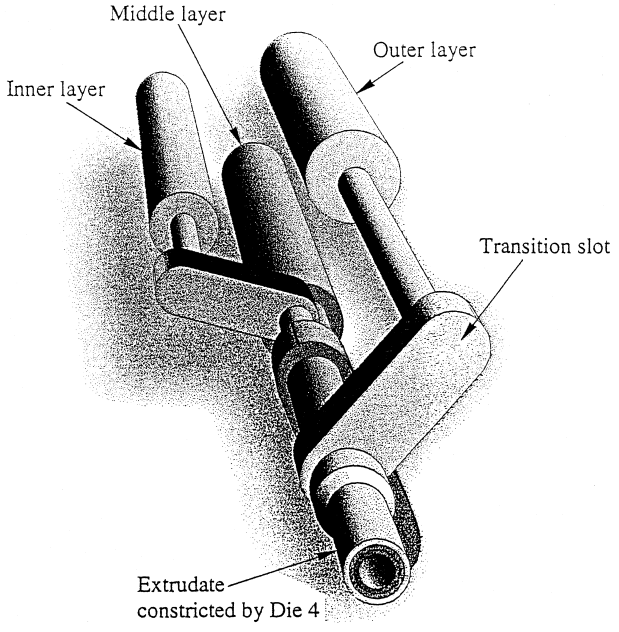

Fig. 2. Illustration of flow streams within the die assembly.

Based on this principle, a die assembly was designed to transfer the three different materials from their respective barrels to form concentric layers around a central mandrel (Pin 1). This was achieved by using an assembly of four dies. The flow paths for the three different materials through the first three dies are illustrated in Fig. 2. The central mandrel (Pin 1) was screwed into the bottom of the barrel block containing the three barrels. Around this pin a die was placed, denoted Die 1 and shown in Fig. 3. Die 1 had two transition holes, a middle hole forming the die land, a transition slot and a thin die wall extension. The middle and outer layer materials were transferred to Die 2 through the transition holes. The inner layer material filled the transition slot and flowed down the central hole around the inner mandrel (Pin 1). The metal tube extension at the bottom of Die 1 forms the mandrel for Die 2 and is denoted Pin 2. This extension preserved the shape of the inner layer extrudate during later layer formation. Dies 2 and 3 had similar structures to Die 1, but with reducing numbers of transition holes. Thus, there are three mandrels (Pins 1–3) associated with three dies (Dies 1–3) when the die set is assembled. The design at this stage would therefore produce three tubes of materials with gaps between each layer as shown in Fig. 4. A final conical die, Die 4 (Fig. 4), compressed the layers to give the final trilayer tube structure around Pin 1. The assembly was held in place by location pins and a clamp ring as shown in Fig. 1.

2.1. Co-extruder dimensions

Having developed a flow scheme and physical structure for the co-extruder, the dimensions of the components were fixed by considering the following criteria.

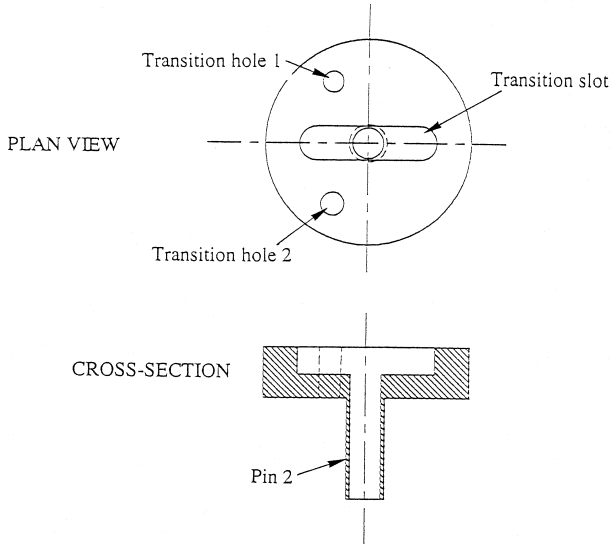

Fig. 3. A schematic drawing of Die 1.

1. Without Die 4 in place, the three layers should travel at the same velocity so that

$$V_{\text{in},x} = V_{\text{mid},x} = V_{\text{out},x} \quad (1)$$

where $V_{i,x}$ is the extrudate velocity for layer i at the exit of the die assembly without Die 4 in place. If one paste travels faster than others, delamination or air bubbles may appear between adjacent layers of the extrudate. $V_{i,x}$ can be calculated by the following equation.

$$V_{i,x} = \frac{A_{i,0}}{A_{i,x}} V_0 \quad (2)$$

where $A_{i,0}$ is the area of the barrel for layer i, $A_{i,x}$ is the toroidal area for layer i exiting Dies 1–3 without Die 4 present. V_0 is the ram speed. As the ram speed and the velocity at the exit of the die assembly are the same for all three layers, the barrel diameters must be different, and Eqs. (1) and (2) can then be re-arranged to give

$$\frac{A_{\text{in},0}}{A_{\text{in},x}} = \frac{A_{\text{mid},0}}{A_{\text{mid},x}} = \frac{A_{\text{out},0}}{A_{\text{out},0}} \equiv \frac{A_{i.0}}{A_{i,x}}. \quad (3)$$

$A_{i,x}$ is normally defined by the final application of the products. In the experimental extruder the layers at the exit of the assembly of dies 1–3 were set to be 1 mm thick, separated by walls 1 mm thick. Hence, the diameters of the barrels were obtained using Eq. (3).

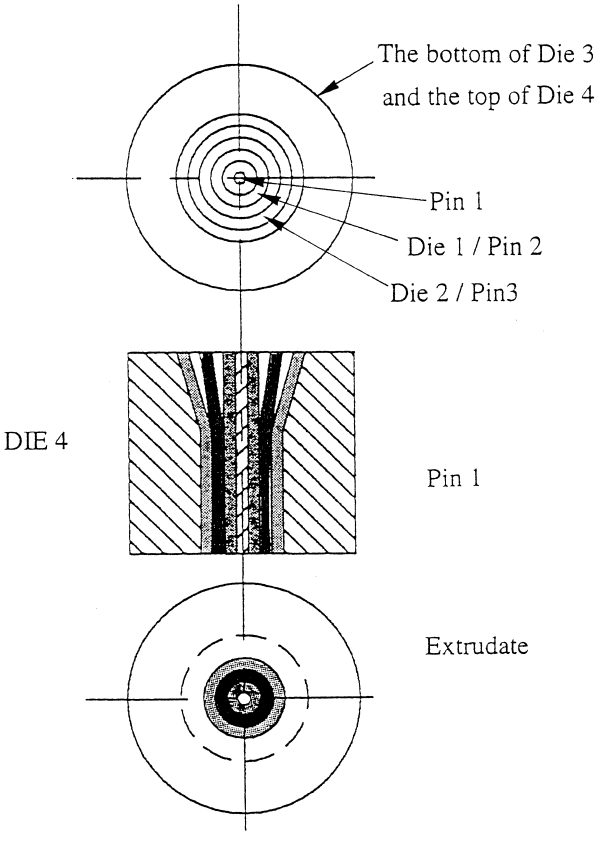

Fig. 4. A schematic drawing of Die 4.

2. Pressure matching without Die 4 in place for different layers ($P_{\text{in}} = P_{\text{mid}} = P_{\text{out}}$) is a natural consequence of the design. The three plungers are forced to move down at the same speed by the load frame. If the resistance on one plunger is higher than that on the others, then that will govern the pressure development. However, any significant imbalance induced by the design or paste mismatching would lead to twisting in the system and potentially mechanical failure. Therefore, the design aimed to give the same pressure drop through each channel for a paste of the same rheology.
3. The pressure drop in the transition slot (P_{B}) should be much less than in the tube land (P_{C}). This pressure difference ensures the slot is fully filled before the paste flows into the tube die land, so that uniform filling of the layers can be achieved.
4. The load required for co-extrusion should not exceed the limit of the load frame and the mechanical design of the barrel and die assembly. The limit here has been set at 100 kN by the load frame used to drive the system. In addition, the load should be as low as possible to keep the extruder construction costs to a minimum.

With the exception of the first criterion, it is pressure drop which is the critical parameter. Pressure drops were predicted before constructing the co-extruder. The cross-sectional areas and lengths of transition slots and transition holes were varied until all the listed criteria 2, 3 and 4 were satisfied. Details of the pressure prediction methods are given in a later section.

2.2. Producing trilayer tubes by the designed co-extruder

Trilayer tubes were successfully produced by the designed co-extruder. Figs. 5 and 6 show samples of two types of trilayer tubes extruded from the design. The outer diameter of the tubes was 6 mm and the inner diameter was 2 mm. The illustrated tubes had well defined roundness, uniform wall thickness and smooth inner and outer surfaces. However, experience showed that successful co-extrusion with this co-extruder was strongly dependent on the paste properties. The paste properties could be adjusted through formulation to allow successful processing.

1. Of prime importance is that the pastes have well matched rheological properties. The dimensions of the co-extruder were determined based on this assumption. Any rheological differences resulted in force differences on the three plungers and velocity differences in Die 4. Force imbalance brought about by different rheological behaviour in the three pastes

caused different flow characteristics, leading to incomplete layer formation in the final extrudate.
2. The formulation and preparation of the pastes is critical, phase migration must be controlled. Uncontrolled phase migration leads to changing rheological properties and can ultimately lead to liquid depletion and unacceptably high extrusion pressures. If the pastes have different stability, then blockage of one channel relative to others may occur leading to potential equipment damage.
3. The pastes should be designed such that shape is retained post extrusion. However, pastes should not be too stiff as high forces may again damage the equipment.

The formulation of pastes with the above behavioural characteristic is discussed by Benbow and Bridgwater.[5]

The extruder had no spider, reducing the potential for defects to be introduced into the flow stream. Most cracks, such as those shown in Fig. 5, occurred during the drying and sintering process. The fixed mandrels (Pins 1–3) would allow cutting in continuous operation.

3. Characterisation of the co-extruder

Pastes can be characterised using an equation model developed by Benbow et al.:[5]

$$P = 2(\sigma_0 + \alpha V)\ln(\frac{D_0}{D}) + 4\frac{L}{D}(\tau_0 + \beta V) \quad (4)$$

where P is the total pressure, required for extrusion through a square entry die of circular cross-section. The paste parameters are σ_0, the bulk yield stress, α, the bulk velocity factor, τ_0, the die wall shear stress and β, the die wall velocity factor. D_0 and D are the diameter of the barrel and die respectively, L is the die length and V the extrudate velocity. This original equation has been extended to deal with non-linear velocity dependence, such that,

$$P = 2(\sigma_0 + \alpha_1 V^m)\ln(\frac{D_0}{D}) + 4\frac{L}{D}(\tau_0 + \beta_1 V^n) \quad (5)$$

where m and n are bulk and wall velocity exponents, respectively, adding two further paste parameters. Note that α_1 and β_1 have different units to α and β in Eq. (4). It has been suggested in the literature[5] that the paste parameters and principles derived from Eq. (4) can be used to calculate the flow in more complex geometries. This principle was applied to predict the pressure drop in flow through the adopted design.

In the co-extruder without Die 4 in place, there are three independent flow paths as shown in Fig. 2. The pressure drops for each of these flow paths are denoted as P_{in}, P_{mid}, and P_{out}, for the inner, middle and outer layer of the tube, respectively, generalised as P_i. Each flow path can be further divided into three sections. The pressure drops into the transition hole, through and along the transition slot and along the tube land are therefore denoted as $P_{A,i}$, $P_{B,i}$ and $P_{C,i}$ respectively.

The pressure drop in transition hole, $P_{A,i}$, for any of the three flow channels comprises two separate pressure drops, one being due to the area change from the barrel to the transition hole, the other due to flow down the transition die land. These two pressure drops are given by:

$$P_{A,i} = 2(\sigma_{0,i} + \alpha_{1,i} V_{1,i}^{m_i})\ln\frac{D_{0,i}}{D_{1,i}} + \frac{4L_{1,i}}{D_{1,i}}(\tau_{0,i} + \beta_{1,i} V_{1,i}^{n_i}) \quad (6)$$

and

$$V_{1,i} = (\frac{D_{0,i}}{D_{1,i}})^2 V_{0,i} \quad (7)$$

where $D_{l,i}$ is the diameter of the transition die and $L_{l,i}$ is its length, $D_{0,i}$ is the diameter of the barrel, $V_{0,i}$ is the ram speed and $V_{1,i}$ is the velocity of paste travelling in the transition die in layer i. Eq. (6) is directly comparable to Eq. (5) as the geometry is essentially the same.

The pressure drop in transition slot $P_{B,i}$ can again be simplified to two sections, one being the pressure required to overcome the shear stress at the wall of the slot land and the other is the pressure required for the paste to deform and flow past the pin associated with layer i to completely fill the slot. This combined pressure drop is given by

$$P_{B,i} = 2\frac{h_i \times L_{2,i} + b_i \times L_{2,i}}{b_i \times h_i}(\tau_{0,i} + \beta_{1,i} V_{2,i}^{n_i}) + \ln(\frac{b_i}{b_i - D_{2,i}})(\sigma_{0,i} + \alpha_{1,i} V_{2,i}^{m_i}) \quad (8)$$

$$V_{2,i} = \frac{\pi D_{0,i}^2}{4 b_i h_i} V_{0,i} \text{ and } V'_{2,i} = \frac{\pi D_{0,i}^2}{4(b_i - D_{2,i})h_i} V_{0,i} \quad (9)$$

where $L_{2,i}$, b_i and h_i are the length, width and height of the transition slot respectively, $D_{2,i}$ is the diameter of the pin i. Velocities of the paste travelling in the slot and in the gap between the slot and the pin are $V_{2,i}$ and $V'_{2,i}$ respectively for layer i.

The calculation of $P_{B,i}$ using Eq. (8) assumes that there is paste flow along the second half of the transition slot and that there is no additional wall friction from the pin, only a contribution due to the cross-sectional area change. This is termed flow pattern I. However, later experimental observation showed the flow pattern to be different to the assumed flow pattern. The true flow path was better represented by that shown in Fig. 7 (Flow pattern II). Therefore, $P_{B,i}$ was recalculated based on this observation and the result is given as $P_{B,i}$(II).

Fig. 5. Al_2O_3/porous Al_2O_3/Al_2O_3 trilayer tube fabricated in the co-extruder (outer diameter 6 mm).

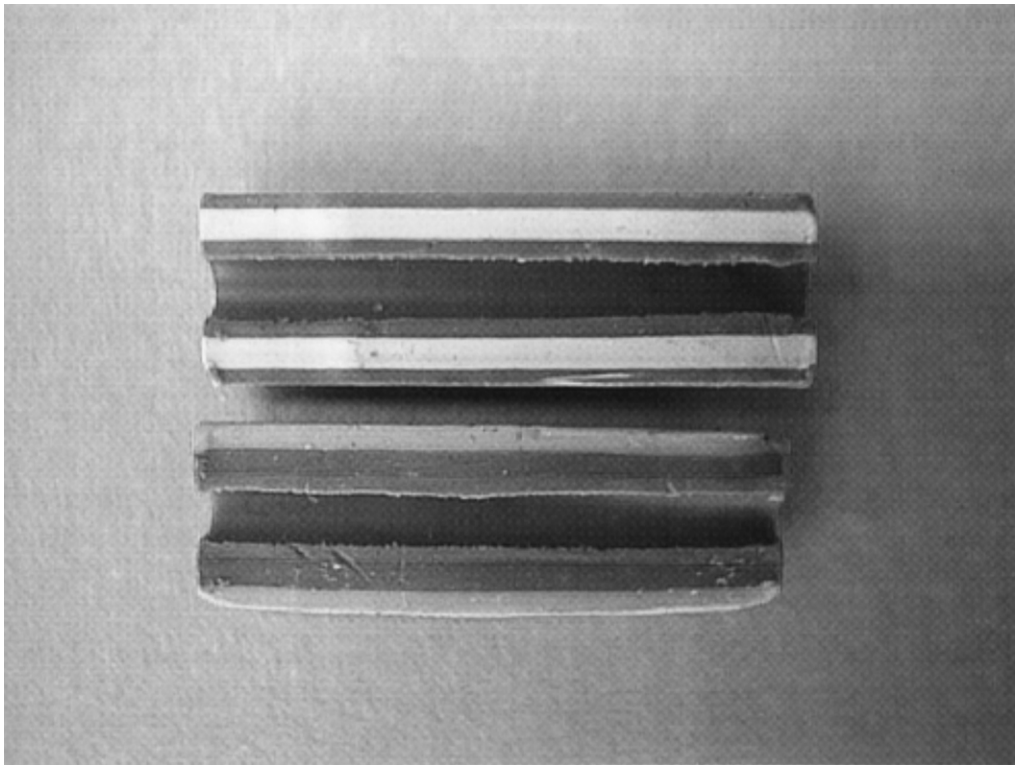

Fig. 6. A picture of a trilayer colourful fun clay tube produced in the co-extruder (outer diameter 6 mm).

$$P_{B,i}(\mathrm{II}) = \frac{h_i \times L_{2,i} + b_i \times L_{2,i}}{b_i \times h_i}(\tau_{0,i} + \beta_{1,i} V_{2,i}^{n_i}) + \ln(\frac{b_i}{b_i - D_{2,i}})(\sigma_{0,i} + \alpha_{1,i} V_{2,i}^{m_i}) + \frac{(\pi D_{2,i} + \pi b_i)h_i + 1/2\pi(b_i^2 - D_{2,i}^2)}{(b_i - D_{2,i})h_i}(\tau_{0,i} + \beta_{1,i} V_{2,i}^{n_i}) \quad (10)$$

The calculation of $P_{C,i}$ is similar to that of $P_{A,i}$ except for the need to consider the influence of the associated pin and the die wall. Initially the flow was considered to be from the total area of the feed slot to the die land configuration and denoted flow pattern I. However, the flow pattern observed later indicated that the flow would be better represented by either the total of the feed slot less the static region (shown in Fig. 7) reducing into the die land orifice (Flow pattern II) or finally to assume that the paste enters the die land orifice as if fed from a barrel of a diameter equivalent to the slot width $b_{2,i}$, such flow being denoted Flow pattern III. Fig. 8 summarizes these three flow patterns. Therefore, the pressure loss in the tube die land was calculated in three ways using:

$$P_{C,i}(\mathrm{I}) = (\sigma_{0,i} + \alpha_{1,i} V_{3,i}^{m,i}) \ln \frac{bL_{2,i} - \pi D_{2,i}^2/4}{\pi(D_{3,i}^2 - D_{2,i}^2)/4} + \frac{4L_{3,i}}{D_{3,i} - D_{2,i}}(\tau_{0,i} + \beta_i V_{3,i}^{m_i}) \quad (11)$$

$$P_{C,i}(\mathrm{II}) = (\sigma_{0,i} + \alpha_{1,i} V_{3,i}^{m_i}) \ln \frac{bL_{2,i}/2 + \pi b_i^2/8 - \pi D_{2,i}^2/4}{\pi(D_{3,i}^2 - D_{2,i}^2)/4} + \frac{4L_{3,i}}{D_{3,i} - D_{2,i}}(\tau_0 + \beta V_{3,i}^{n_i}), \quad (12)$$

$$P_{C,i}(\mathrm{III}) = (\sigma_{0,i} + \alpha_{1,i} V_{3,i}^{m_i}) \ln \frac{\pi b_i^2 - \pi D_{2,i}^2}{\pi(D_{3,i}^2 - D_{2,i}^2)/4} + \frac{4L_3}{D_{3,i} - D_{2,i}}(\tau_0 + \beta V_{3,i}^{n_i}) \quad (13)$$

where the diameter of the die is $D_{3,i}$ and its length is $L_{3,i}$, and the extrudate velocity within the die is $V_{3,i}$.

The pressure drop required for co-extrusion without Die 4 in place can therefore be calculated by:

$$P_{i,(\mathrm{I})} = P_{\mathrm{A},i} + P_{B,\mathrm{I}}(\mathrm{I}) + P_{C,\mathrm{I}}(\mathrm{I}) \quad (14)$$

or

$$P_{i,(\mathrm{II})} = P_{\mathrm{A},i} + P_{B,\mathrm{I}}(\mathrm{II}) + P_{C,\mathrm{I}}(\mathrm{II}) \quad (15)$$

or

$$P_{i,(\mathrm{III})} = P_{\mathrm{A},i} + P_{B,\mathrm{I}}(\mathrm{III}) + P_{C,\mathrm{I}}(\mathrm{III}) \quad (16)$$

The pressure drop in Die 4, P_w is the sum of three components ($P_w = P_1 + P_2 + P_3$). P_1 is the pressure drop due only to the change in cross-sectional area. P_2 and P_3 are the pressure drops that are required to overcome the wall resistance to flow along the perimeter of the cylindrical die land and the conical die land, respectively. This gives

$$P_1 = (\sigma_0 + \alpha_1 V_4^m) \ln \frac{R_4^2 - R_6^2}{R_5^2} \quad (17)$$

$$P_2 = (\tau_0 + \beta_1 V_4^n)(\frac{2R_5 L_4 + 2R_6 L_5)}{R_5^2 - R_6^2} \quad (18)$$

$$\int_0^{P_3} P_3 = \int_{R_5\cot\theta}^{R_4\cot\theta} \frac{2\tau_0 + 2\beta_1[\frac{\pi(R_5^2 - R_6^2)V_4}{\pi(z^2\tan^2\theta - R_6^2)}]^n}{z\tan\theta - R_6} dz \quad (19)$$

where R_4 is the entry radius of Die 4, R_5 is the exit radius of Die 4, R_6 is the radius of Pin 1, V_4 is the extrudate velocity, L_4 is the length of the cylindrical land of Die 4, L_5 is the length of Pin 1 beyond Die 3 ($L_5 > L_4$), θ is the cone half-angle, and z is the paste flowing direction.

Finally, the total load required for co-extrusion can be obtained by:

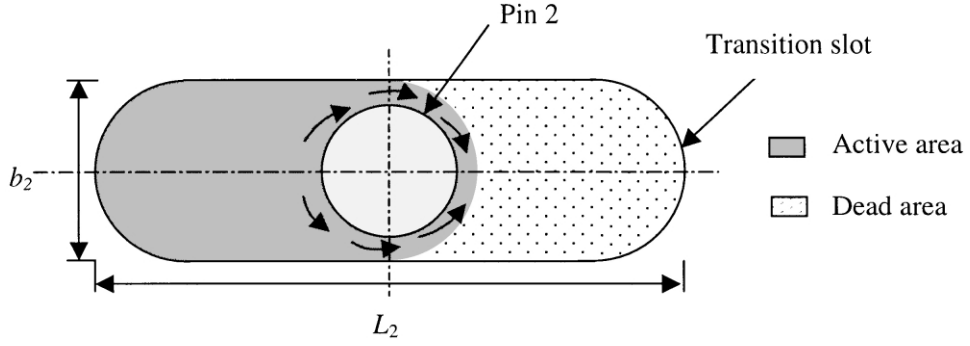

Fig. 7. Illustration of nomenclature used in the $P_{\mathrm{B(II)}}$ calculation for middle flow stream.

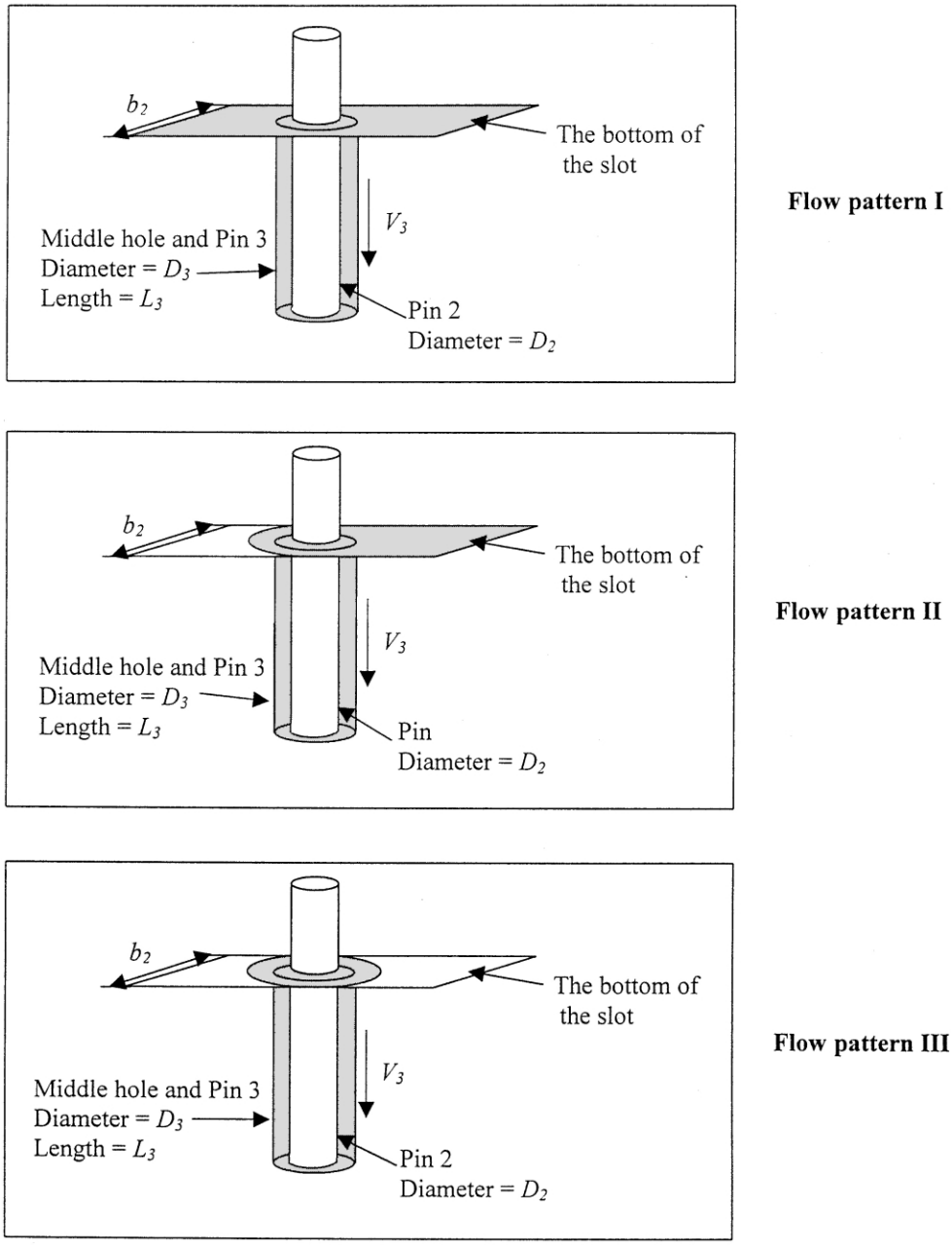

Fig. 8. Illustration of the middle flow stream (shaded areas) used in the calculation of P_C.

$$F = P_{\text{in}} \times A_{\text{in},0} + P_{\text{mid}} \times A_{\text{mid},0} + P_{\text{out}} \times A_{\text{out},0} + P_w \times \left(A_{\text{in},0} + A_{\text{mid},0} + A_{\text{out},0}\right) \quad (20)$$

where $A_{i,0}$ is the generalised area of barrel i. Details of the whole computing procedures are given by Liang.[6]

3.1. Model verification

To demonstrate the applicability of the model, pressure drop was determined when passing an alumina paste through the co-extruder at a ram speed of 2 mm/s. The paste was characterised using a ram extruder attached to a 100 kN load frame (Model 1195 Instron, UK). The barrel was 25.4 mm in diameter, to which was attached one of three dies. The dies were all 3 mm in diameter with L/D ratios of 2, 4 and 8. Extrusion pressures were measured at six extrudate velocities for each die. The data was used to solve Eq. (5). Table 1 lists the paste formulation and paste rheological parameters. Table 2 shows the calculated results for co-extrusion for each die section, accounting for the three flow patterns defined by Eqs. (14)–(16). The predictions from the

three flow patterns gave similar results, the difference being within 5%. This result shows that the difference caused by uncertainty within the transition slot is of little consequence to the overall pressure drop. Therefore, only one flow pattern, flow pattern I, was applied for predictions for different paste formulations and of course the original extruder design. In general, three flow paths without Die 4 in place are predicted to generate similar pressure drops ($P_{in} \approx P_{mid} \approx P_{out}$). The pressure distribution in each flow path is also shown in Table 2. For all three paths, the pressure drops in the slot are much lower than those in the tube die land ($P_B \ll P_C$). The estimated load required for co-extruding this paste under the selected operating conditions was around 25 kN, which is much lower than the limit of the load frame. In summary, the design adopted for the co-extruder satisfied to the required level all criteria outlined earlier.

The adopted design gave good continuity with the three independent barrels, it ensured that trilayer ceramic tubes could be produced semi-continuously, meaning that production ceased only when the barrels were empty. In the future these independent barrels used in the experimental extruder could be refilled automatically or the barrels could be replaced by twin screw extruders which give positive displacement. Though problems with producing matched flow rates are envisaged in twin screw systems without close control and extensive development.

3.2. Comparison of predicted and measured pressure drops of five pastes through the co-extruder

To further verify the applicability of the calculation, five pastes were prepared for flow characterisation through the co-extruder. Three pastes were of one formulation group, denoted Type A, their behaviour modified by different liquid contents. The fourth paste, Type B, had a similar formulation to Paste A(2) with addition of 0.07 wt.% glycerol. The last paste, Type C, was "colourful fun clay", a modelling dough. The formulations of these pastes, where available, are listed in Table 3.

The rheological properties of the five pastes were measured by capillary rheometer as before and analysed using Eqs. (4) and (5).[5] Fig. 9 shows the pressure drop and extrudate velocity relationship for paste A(2). All pastes exhibited pseudo-plastic behaviour and hence the best fit was always obtained using Eq. (5). The measured rheological parameters of the pastes are listed in Tables 4 and 5 for the two equations. The following reasons are suggested for the generation of the negative α values reported for the "colourful fun clay". In the long die frictional heating effects may have softened the material during the extrusion. Alternatively, the higher pressure generated during long die extrusion may have resulted in material break down or re-arrangement, so that the material became more fluid.

Table 1
Paste formulation and paste rheological parameters for the Al_2O_3 paste used in the development of the co-extruder

Paste contents	Paste parameters	
$Al_2O_3$100.0 g	$\sigma_0$0.30 MPa	τ_0 0 MPa
Binder 8.0 g	α_1 11.09 MPa s^{-m}	β_1 11.35 MPa s^{-n}
Solvent 14.4 g	m 0.41	n 0.46

Table 2
Predicted loads and pressure drops for the Al_2O_3 paste (Table 1) in the co-extruder

Load (kN)	Flow pattern I	Flow pattern II	Flow pattern III						
Inner	3.21	3.15	3.16						
Middle	6.79	6.70	6.59						
Outer	9.25	10.3	10.1						
Die 4	6.07	6.07	6.07						
Total	25.3	26.2	26.0						
Pressure (MPa)	$P_{i(I)}$	$P_{i(II)}$	$P_{i(III)}$	$P_{A,i}$	$P,i_{B(I)}$	$P_{B,i(II)}$	$P_{C,i}$	$P_{C,i(II)}$	$P_{C,i(III)}$
Inner	28.4	27.9	27.9	0.30	3.76	3.67	24.3	23.9	24.0
Middle	26.7	26.4	25.9	3.37	6.32	6.41	17.0	16.6	16.1
Outer	22.3	24.8	24.4	5.18	6.32	9.26	10.8	10.3	9.99

Table 3
Paste formulations

Type	A(1)	A(2)	A(3)	B	C
Al_2O_3 (wt.%)	82.4	81.7	80.9	81.6	
Binder (wt.%)	6.3	6.5	6.8	6.5	Commercial
Solvent (wt.%)	11.3	11.8	12.3	11.8	colour fun clay
Glycerol (wt.%)	0	0	0	0.1	
Liquid content (wt.%)	17.6	18.3	19.1	18.4	

Table 4
Paste parameters from four-parameter characterisation

	A(1)	A(2)	A(3)	B	C
σ_0 (MPa)	1.84	0.847	0.67	0.35	0.24
α (MPa s m^{-1})	276.6	100.9	142.7	38.1	−14.6
τ_0 (MPa)	0.69	0.406	0.24	0.34	0.094
β (MPa s m^{-1})	106.6	90.6	50.1	67.3	19.34

All the pastes were passed through the co-extruder at three different extrusion velocities. The forces required were measured and are reported in Tables 6 and 7.

The predicted values in Table 6 were calculated from the paste parameters derived from Eq. (5) and reported in Table 5 using Eqs. (6)–(20). The error values reported indicate the degree of fit between the predictions and the experimental data. For pastes of type A, the predicted forces were overestimated, the difference being within 15%. For pastes of types B and C, the predicted values were lower than the experimental data, the error ranging from −20 to −30%. In general, the predicted data follow the same trend as the measured values though the closeness of the fit is dependent on composition and plasticity of the pastes. Errors are generated in fitting Eq. (5) to the capillary data and these errors compromise the predictions in the co-extruder. Some gross simplifications are made in the prediction of flow in the co-extruder and this further contributes to the deviation between the measured and predicted values. Given these constraints, the usefulness of the approach in design is demonstrated.

Table 5
Paste parameters from six-parameter characterisation

	A(1)	A(2)	A(3)	B	C
σ_0 (MPa)	0.97	0.30	0.15	0	0.85
α_1 (MPa s^{-m})	50.45	11.09	21.58	3.20	−1.20
m	0.55	0.41	0.51	0.31	0.09
τ_0 (MPa)	0	0	0	0	0
β_1 (MPa s^{-n})	10.45	11.35	6.01	7.83	2.28
n	0.38	0.46	0.44	0.43	0.44

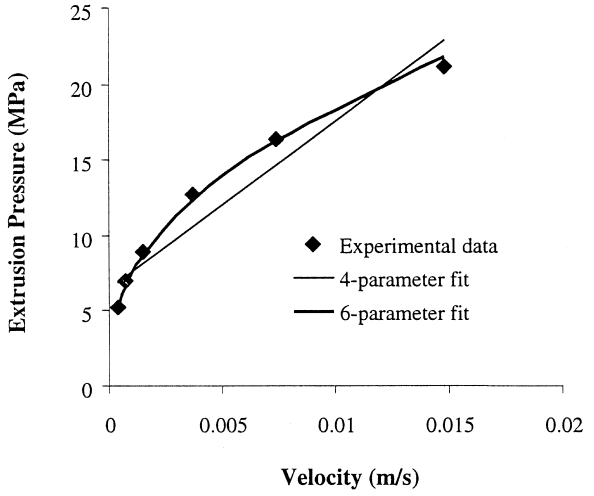

Fig. 9. Pressure velocity curve and model fits for paste A(2) at $L/D = 8$.

Table 6
Prediction from six-parameter characterisation and experimental measurement

Error (%) = (Prediction − Experiment)/Experiment × 100				
l	Extrudate velocity (m/s)	1.04E-3	5.19E-4	2.60E-4
A(1)	Experiment (kN)	44.6	32.8	25.3
	Prediction (kN)	45.3	36.0	29.1
	Error (%)	2	10	15
Paste type	Extrudate velocity (m/s)	1.04E-3	5.19E-4	2.60E-4
A(2)	Experiment (kN)	25	18.75	14.5
	Prediction (kN)	25.3	19.2	14.7
	Error (%)	1	2	1
Paste type	Extrudate velocity (m/s)	1.04E-3	5.19E-4	2.60E-4
A(3)	Experiment (kN)	14.1	10.8	8.3
	Prediction (kN)	15.7	11.7	8.9
	Error (%)	11	9	7
Paste type	Extrudate velocity (m/s)	1.04E-3	5.19E-4	2.60E-4
B	Experiment (kN)	23.3	18.1	15.0
	Prediction (kN)	18.9	14.3	10.9
	Error (%)	−19	−21	−27
Paste type	Extrudate velocity (m/s)	1.04E-3	5.19E-4	2.60E-4
C	Experiment (kN)	8.6	7.0	6.0
	Prediction (kN)	6.36	5.34	4.63
	Error (%)	−26	−24	−23

Table 7
Prediction from four-parameter characterisation and experimental measurement

Error (%) = (Prediction − Experiment)/Experiment × 100				
Paste type	Extrudate velocity (m/s)	1.04E-3	5.19E-4	2.60E-4
A(1)	Experiment (kN)	44.6	32.8	25.3
	Prediction (kN)	59.4	57.5	56.5
	Error (%)	33	75	123
Paste type	Extrudate velocity (m/s)	1.04E-3	5.19E-4	2.60E-4
A(2)	Experiment (kN)	25	18.75	14.5
	Prediction (kN)	34.2	32.8	32.0
	Error (%)	37	75	121
Paste type	Extrudate velocity (m/s)	1.04E-3	5.19E-4	2.60E-4
A(3)	Experiment (kN)	14.1	10.75	8.3
	Prediction (kN)	21.2	20.2	19.8
	Error (%)	50	88	139
Paste type	Extrudate velocity (m/s)	1.04E-3	5.19E-4	2.60E-4
B	Experiment (kN)	23.25	18.1	15.0
	Prediction (kN)	28.3	25.0	24.5
	Error (%)	22	38	63
Paste type	Extrudate velocity (m/s)	1.04E-3	5.19E-4	2.60E-4
C	Experiment (kN)	8.6	7.0	6.0
	Prediction (kN)	7.91	7.72	7.65
	Error (%)	−8	10	28

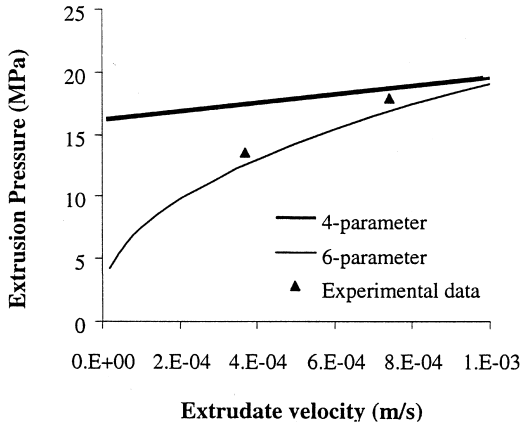

Fig. 10. Fig. 9 expanded at low velocities.

The predicted values in Table 7 were calculated using the paste parameters derived from Eq. (4). The calculation follows the same procedures described above, except m and n were set to 1 for the whole calculation and σ_0, α, τ_0 and β adjusted accordingly. In this case, fit between prediction and experiment was poor, some errors being greater than 100%. For these reasons the four-parameter characterisation can not be used to analyse the flow behaviour of such pseudo-plastic pastes, especially at low extrudate velocities in such complex geometries. Fig. 10 shows the pressure drop in a capillary at low velocities for paste A(2). It can be seen that a large error is introduced by the application of Eq. (4), which results in poor load predictions for the co-extrusion process.

4. Conclusions

The design procedures for a co-extruder are reported. A co-extruder has been constructed using these principles and used to produce trilayer tubes from ceramic pastes. The success of the design relies on velocity, rheology and pressure matching in the different layers. Flow in the designed co-extruder was characterised by a physically based model. The model, when used in its more complex form gave reasonable agreement with measured values provided the paste was not highly plastic in nature. The alternative reduced parameter characterisation method could not be used to analyse the flow behaviour of pseudo-plastic pastes, especially at low extrudate velocities.

Acknowledgements

The authors would like to thank the ORS scheme and the School of Chemical Engineering for the funding to carry out this work. The EPSRC is acknowledged for its funding of the IRC in Materials for High Performance Applications, where this work was carried out.

References

1. Van Hoy, C., Barda, A., Griffith, M. and Halloran, J. W., Microfabrication of ceramics by co-extrusion. *Journal of the American Ceramic Society*, 1998, **81**(1), 152–158.
2. Liang, Z. and Blackburn, S., Co-extrusion of multilayer tubes. *British Ceramic Proceedings*, 1998, **58**, 113–124.
3. Shannon, T. and Blackburn, S., The production of alumina/zirconia laminated composites by co-extrusion. *Ceramic Engineering and Science Proceedings*, 1995, **16**, 1115–1120.
4. Doshi, S. R., Charrier, J. M. and Dealy, J. M., A co-extrusion process for the manufacture of short-fibre-reinforced thermoplastic pipe. *Polymer Engineering and Science*, 1988, **128**(15), 964–973.
5. Benbow, J. J. and Bridgwater, J., Die design and construction. In *Paste Flow and Extrusion*, ed. J. R. Crookall, M. C. Shaw and N. P. Suh. Clarendon Press, Oxford, 1993, pp. 83–97.
6. Liang, Z., Design and characterisation of a co-extruder. In *Co-extrusion of Multilayer Tubes*, PhD thesis, The University of Birmingham, 1999.